

## Structure and infrared emissivity of polyimide/mesoporous silica composite films

Lin Baoping<sup>a,b,\*</sup>, Tang Jinan<sup>a</sup>, Liu Hongjian<sup>a</sup>, Sun Yueming<sup>a</sup>, Yuan Chunwei<sup>b</sup>

<sup>a</sup>Department of Chemistry and Chemical Engineering, Southeast University, Nanjing 210096, PR China

<sup>b</sup>Key Laboratory of Molecular and Biomolecular Electronics of Ministry of Education, Nanjing 210096, PR China

Received 24 October 2004; received in revised form 6 December 2004; accepted 7 December 2004

### Abstract

Polyimide/mesoporous silica composite films were prepared by direct mixing of polyamic acid solution and silylated mesoporous silica particles, or by condensation polymerization of dianhydride and diamine with silylated mesoporous silica particles in *N,N*-dimethylacetamide, followed with thermal imidization. Structure and glass transition temperatures of the composite films were measured with FTIR, SEM, EDX, XPS and DMTA. The results show that the silylated mesoporous silica particles in the composites tend to form the aggregation with a strip shape due to phase separation. The composite films exhibit higher glass transition temperature as comparing with that of pure polyimide. It is found that the composite films present lower infrared emissivity value than the pure polyimide and the magnitude of infrared emissivity value is related to the content of silylated mesoporous silica in the composite films. Inhibiting actions of silylated mesoporous silica on infrared emission of the composite films may be owing to presence of nanometer-scale pores in silylated mesoporous silica.

© 2004 Elsevier Inc. All rights reserved.

**Keywords:** Polyimide; Mesoporous silica; Composite; Infrared emissivity

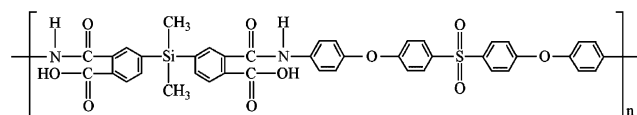
The general class of materials called hybrid inorganic–organic composites has garnered concerted research efforts for many years [1,2]. Recently, inorganic–organic mesostructured materials present a wide range of scientific and practical interests. The inorganic–organic mesostructured materials composed of hard and soft materials synergistically intertwined to provide both useful functionality and mechanical integrity [3]. The interaction between the inorganic and organic compositions through physical force and chemical bond is important as a method for controlling the structure and properties of the inorganic–organic mesostructured materials.

In this communication, we prepared polyimide (Structure 2)/mesoporous silica composite films by direct mixing of polyamic acid (Structure 1) solution and silylated mesoporous silica particles under the mechanical stirring, or by condensation polymerization of dianhydride and diamine with silylated mesoporous silica particles in *N,N*-dimethylacetamide (DMAc), followed with thermal imidization. The structure and infrared emissivity of polyimide/mesoporous silica composite films were investigated.

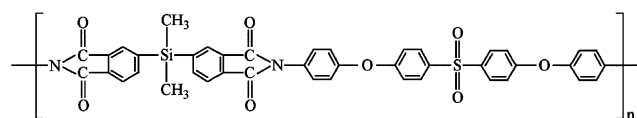
The synthesis of mesoporous silica was achieved in the presence of cetylamine template in water with ethanol as a cosolvent [4]. In a typical preparation, tetraethyl orthosilicate (27.8 mmol) was dropwisely added under vigorous stirring to a solution of cetylamine (7.5 mmol) in ethanol (19.2 ml) and deionized water (16.8 ml). After dripping out, the reaction mixture was aged at ambient temperature for 18 h, and resulting hexagonal mesoporous silica (HMS) was air-dried at

\*Corresponding author. Key Laboratory of Molecular and Biomolecular Electronics of Ministry of Education, Department of Chemistry and Chemical Engineering, Si Pailou 2, Nanjing city, Jiangsu province 210096, China. Fax: +0086 25 83793171.

E-mail address: [lbp@seu.edu.cn](mailto:lbp@seu.edu.cn) (L. Baoping).



Structure 1.

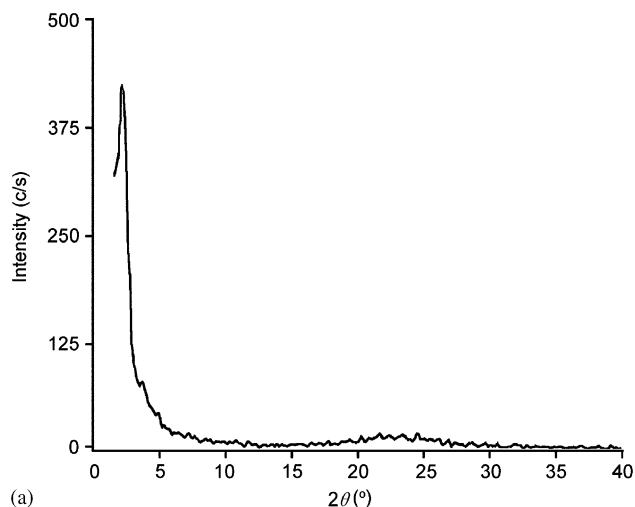


Structure 2.

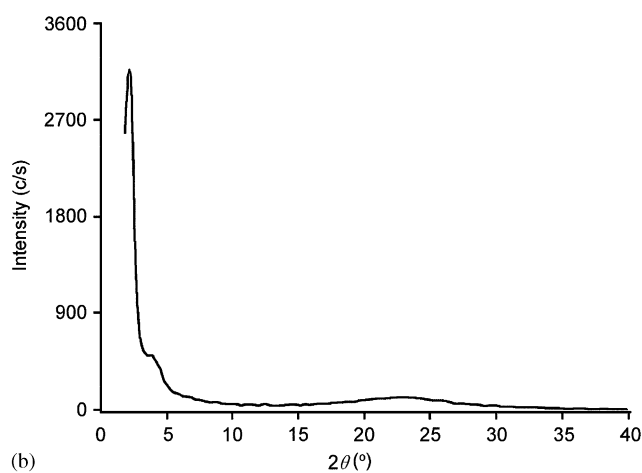
80 °C. Then cetylamine template was removed by extracting 2 g of the air-dried mesoporous silica with 300 ml of hot ethanol for 24 h, and the product was filtered and washed with 100 ml of hot ethanol two times. Finally, the product (denoted HMS–EE) was dried at 80 °C for 1.5 h.

Silylation of HMS–EE was performed by the method described in literature [5] as follows. One gram amount of HMS–EE (dry weight), 40 ml of xylene, 0.16 mmol of 3-(trimethoxysilyl)propyl methacrylate (KH-570) and a magnetic stirrer were enclosed in a bottle and purged with N<sub>2</sub>. After the mixture was stirred for 30 min, the suspended solution was refluxed for 1 h. Then the sample was filtered over a Buchner filter. The silylated mesoporous silica (designated S-HMS–EE) was washed with dry propanone three times, and then dried at 80 °C in vacuo.

The presence of methacrylate groups on surface of S-HMS–EE is confirmed by Fourier transform infrared spectroscopy (FTIR, Nicolet Magna-IR 750 spectrometer). Powder X-ray diffraction (XRD, Shimadzu XD-3A diffractometer) patterns (Fig. 1) of HMS–EE and S-HMS–EE show that all patterns are similar and exhibit a single diffraction peak corresponding to *d* spacing of 4.3 and 4.0 nm, respectively. Higher order Bragg reflections of the hexagonal structure are not resolved. The absence of additional reflections of the lamellar phase could be attributed to the limited order in the lamellar framework of this silicate [6]. The silylation of mesoporous silica by KH-570 increases the intensity of diffraction peak. The intensity of the *d*<sub>100</sub> diffraction of S-HMS–EE is higher than that of HMS–EE about seven point five times. This is ascribed to the increase of regularity of silylated mesoporous silica. Scanning electron microscopy (SEM, LEO 1530VP microscope) images (Fig. 2) reveal that the as-synthesized S-HMS–EE sample consists of many worm-like particles, which are aggregated into sphere-like macrostructures with the diameter of several hundred nanometers to 1 μm.



(a)



(b)

Fig. 1. Powder X-ray diffraction patterns for mesoporous SiO<sub>2</sub> (a), and silylated mesoporous SiO<sub>2</sub> (b).

The polyamic acid was synthesized by mixing an equivalence of relevant *bis*(3,4-dicarboxyphenyl)dimethylsilane dianhydride (SIDA) and 4,4'-*bis*(4-aminophenoxy)diphenyl sulfone (BAPDS) at room temperature in DMAc solution, and reacting for 24 h. The quantitative powders of S-HMS were added into the solution of polyamic acid in DMAc with vigorous stirring. After the mixing process completed, the mixture was cast on a clear glass plate. After the coat on a glass plate was gently baked at 60 °C in vacuo for 1 h, with most of solvent withdrawn, the gel film was formed. To evacuate the DMAc remaining in the film, polyamic acid/S-HMS gel film was continuously treated at 100 °C and 150 °C in vacuo for 1 h, respectively. Finally, the imidization of polyamic acid/S-HMS–EE thin film was performed in steps for 1 h at 200 °C and 1 h at 280 °C. The resulting polyimide/S-HMS–EE thin films designed PI-1-m and PI-10-m contain 1% (wt/wt) and 10% (wt/wt) of S-HMS–EE, respectively. At the same time, polyimide/S-HMS–EE composite films were also prepared by mixing an equivalence of relevant SIDA and

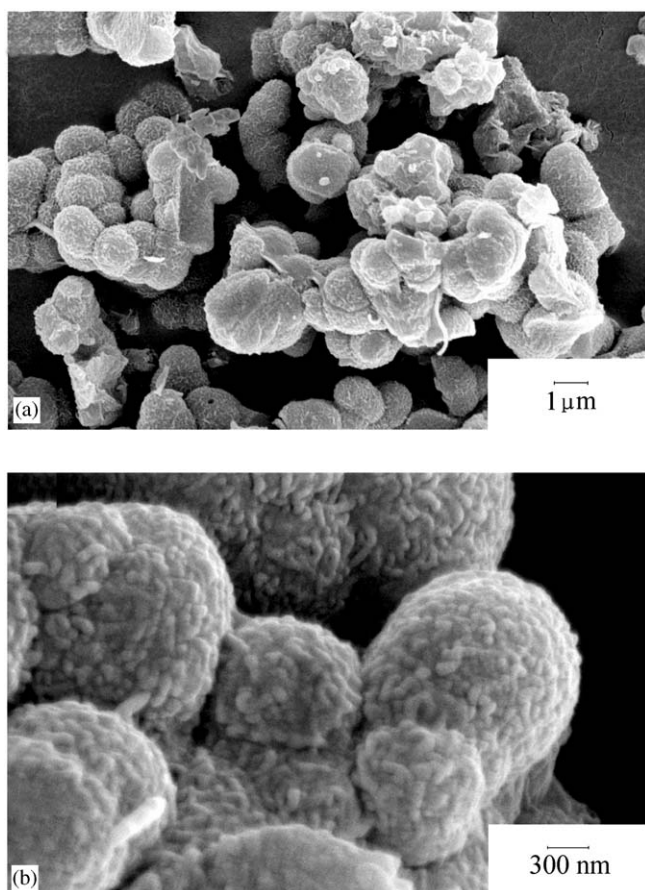


Fig. 2. Scanning electron micrographs of as-synthesized silylated mesoporous silica at different magnifications.

BAPDS with the quantitative S-HMS-EE powders at room temperature in DMAc solution, and reacting for 24 h and followed with thermal imidization. The conditions preparing films are the same as those of PI-1-m and PI-10-m. The both films prepared by this method are denoted as PI-1-c (1% S-HMS-EE, wt/wt) and PI-10-c (10% S-HMS-EE, wt/wt). The thickness of the composite films is about 50 μm. ATR-FTIR (Attenuated total reflection-Fourier transform infrared spectroscopy) spectra show that the polyamic acid within all polyimide/S-HMS-EE composite films is completely converted into polyimide.

Silylated mesoporous silica can be conveniently dispersed in DMAc to form a semi-transparent and uniform sol solution. Therefore, S-HMS-EE can be uniformly dispersed in a solution of polyamic acid in DMAc. Generally, in the system of silica-polyimide, the addition of small amounts of coupling agent can evidently improve the miscibilization of silica-polyimide mixtures and inhibit the aggregation of silica particles; silica in polyimide film exhibits sphere-like particle shape [7]. Whereas in polyimide/S-HMS-EE composite films, SEM studies of cross-section of free-standing PI-10-m composite films reveal that aggregation of

S-HMS-EE particles occur due to phase separation of polyimide and silylated mesoporous silica, and forms a strip shape (Fig. 3a and b). SEM studies for cross-section of the PI-10-c composite film also reveal that S-HMS-EE particles coalesce to form a strip aggregation, which is similar to the PI-10-m composite film (Fig. 3c), but the regularity of the aggregation is poorer. This may be ascribed to the long-time stirring that partially destroys the framework of silylated mesoporous silica.

Energy dispersive X-ray spectroscopy (EDX, OXFORD INSTRUMENTS INCA x-sight) measurement

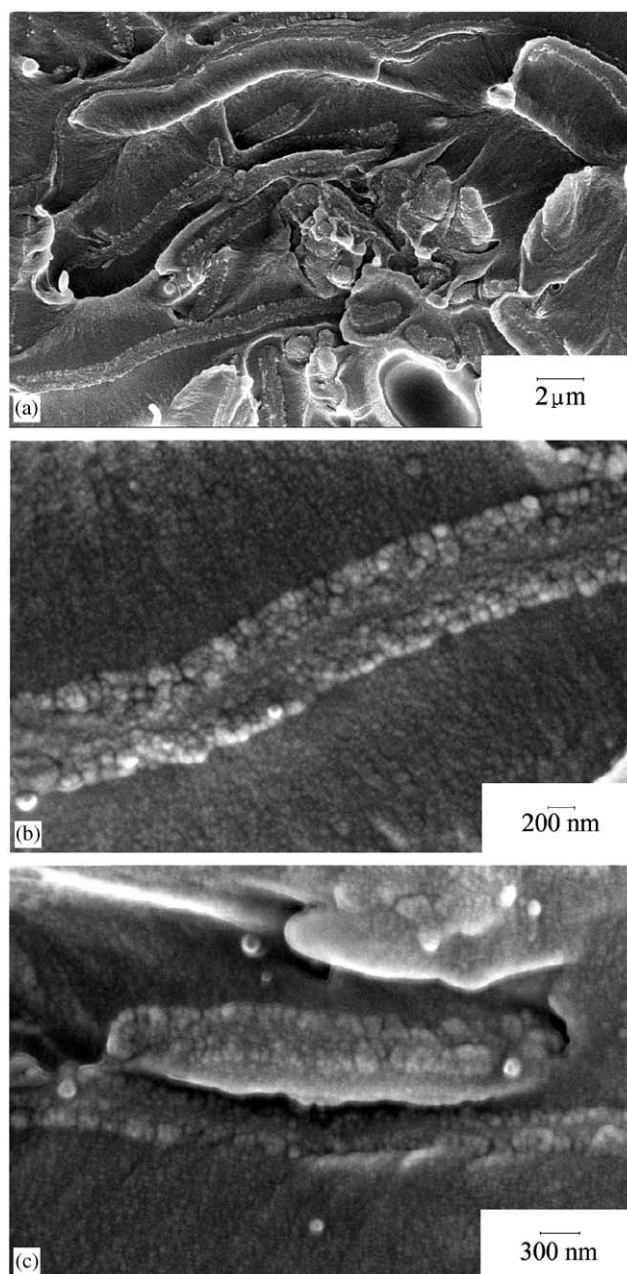


Fig. 3. Cross section scanning electron micrographs of polyimide/S-HMS-EE composite films: (a) and (b) PI-10-m at different magnifications; (c) PI-10-c.

and quantitative elemental analysis made on different domains of the polyimide/S-HMS-EE composite films show the expected corresponding element signs. S element sign is not found on aggregation of S-HMS-EE with a strip shape; however, it is found in the area outside the aggregation. This confirms that the aggregation consists of silylated mesoporous silica particles. In addition, Local EDX analysis indicates that the distribution of the elements is much the same on the different domains of the aggregation of S-HMS-EE particles.

Dynamic mechanical analysis was performed on a Rheometric Scientific Mark V, dynamic mechanical thermal analyzer (DMTA). The run conditions were conducted at a frequency of 1 Hz and a heating rate of 3 °C/min from –100 to 300 °C in air. The results are tabulated in Table 1. The glass transition temperatures ( $T_g$ ) of the composites are affected by incorporation of S-HMS-EE particles into the polyimide matrix. The  $T_g$  of the composites prepared by direct mixing of polyamic acid solution and S-HMS-EE particles increases with increasing the content of S-HMS-EE, however the  $T_g$  of the composite films prepared by the condensation polymerization of SIDA and BAPDS with S-HMS-EE particles decreases with the increase of the content of the S-HMS-EE particles. This fact may reflect that morphology of the composite films varies with the content of silylated mesoporous silica and preparing methods. The magnitude of  $\tan \delta$  at  $T_g$  is a measure of the energy-damping characteristic of the material and can be related to the ease at which polymer chains move in concert through the glass transition [8]. With the increase of the content of S-HMS-EE, the magnitude of  $\tan \delta$  at  $T_g$  decreases. This result is consistent with varying trend of the magnitude of  $\tan \delta$  at  $T_g$  for a particle filled system.

The beta relaxation,  $\beta$ , occurs below the  $T_g$ , is associated with local bond rotations and molecular segment motions along the polymer backbone, and the magnitude of this relaxation is proportional to the concentration of segments contributing to the relaxation. In our experiments, when the content of S-

HMS-EE in the composite films is 1%,  $\tan \delta$  values at the  $\beta$  transition increase in comparison with the pure polyimide, however when the content of S-HMS-EE in the composite films increases to 10%,  $\tan \delta$  values at the  $\beta$  transition decrease. On the other hand, incorporation of S-HMS-EE particles into the polyimide results in increasing of the  $\beta$  transition temperature.

Several kinds of materials with low infrared emissivity, such as composite ceramics of  $\text{Fe}_2\text{O}_3\text{-MnO}_2\text{-Co}_2\text{O}_3\text{-CuO}$ , sol-gel indium tin oxide films of various composition, silicon-containing polyimide/BaTiO<sub>3</sub> nanocomposite films et al have been investigated [9–12]. But little is known about infrared emissivity of polymer/S-HMS-EE composites. Infrared emissivity values and spectra of polyimide/S-HMS-EE composite films were recorded on a Nicolet Magna-IR 750 spectrometer equipped with an FTIR emission accessory at 80 °C. The representative infrared emissivity spectra of pure polyimide, PI-1-c and PI-10-c composite films are shown in Fig. 4. It is clearly seen that silylated mesoporous silica inhibit strongly infrared emission of the composite films.

The integrating values ( $\varepsilon_{\text{TE}}$ ) of infrared emissivity in the range of 8–14  $\mu\text{m}$  are summarized in Table 1. The  $\varepsilon_{\text{TE}}$  of the composites varies with the content of S-HMS-EE in the composites. The  $\varepsilon_{\text{TE}}$  of the composites prepared by direct mixing of polyamic acid solution and S-HMS-EE particles increases with increasing the content of S-HMS-EE, however that prepared by condensation polymerization of SIDA and BAPDS with

Table 1  
Components and properties of polyimide/mesoporous silica composite films

Sample codes	$T_g$ ( $\alpha$ )		$\beta$		Infrared emissivity ( $\varepsilon_{\text{TE}}$ at 8–14 $\mu\text{m}$ )
	(°C)	$\tan \delta$	(°C)	$\tan \delta$	
PI-0 <sup>a</sup>	238	1.486	60	0.043	0.521
PI-1-m	245	1.251	63	0.051	0.418
PI-10-m	246	0.703	72	0.032	0.457
PI-1-c	247	1.446	70	0.056	0.392
PI-10-c	245	0.831	70	0.053	0.356

<sup>a</sup>Pure polyimide prepared by SIDA and BAPDS.

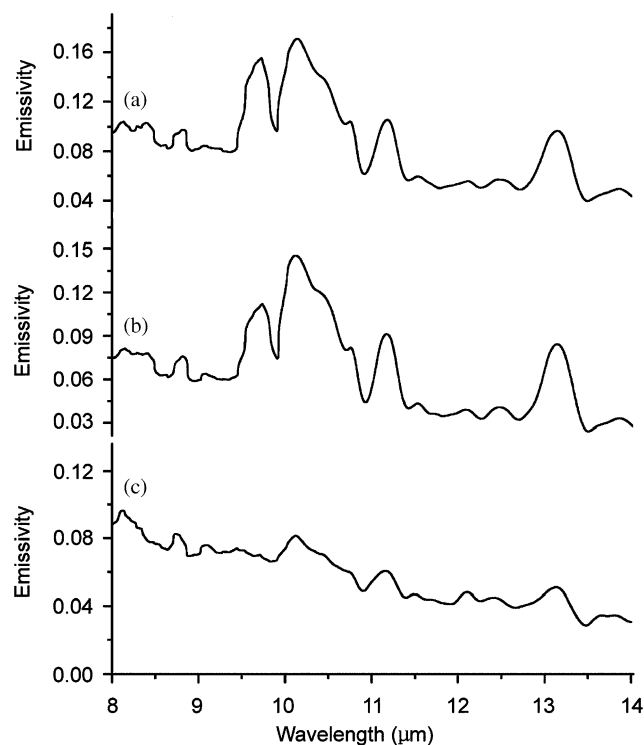


Fig. 4. Infrared emissivity spectra of polyimide/S-HMS-EE composite films: (a) pure polyimide; (b) PI-1-c; (c) PI-10-c.

S-HMS-EE particles decreases with increasing of the content of S-HMS-EE in the composites. The differences of structure and morphology of composite films prepared by different method result in  $\epsilon_{TE}$  values of composite films with preparing method to present different varying tendency. Interfacial interactions between the polyimide and S-HMS-EE components are hardly found by measurement of X-ray photoelectric spectra (XPS, VG ESCALAB-MKII). Therefore, inhibiting actions of silylated mesoporous silica on infrared emission of the composite films may be owing to presence of nanostructure pores in S-HMS-EE. These nanostructure pores absorb partially energy emitted by the composite films in the range of 8–14  $\mu\text{m}$ .

In summary, the polyimide/mesoporous silica composite films have been produced based on mixing of the polyamic acid and silylated mesoporous silica particles under the mechanical stirring, or by condensation polymerization of dianhydride and diamine with silylated mesoporous silica particles in DMAc, followed with thermal imidization. Silylated mesoporous silica particles in the composites tend to form the aggregation with a strip shape due to phase separation. The composite films obtained by this approach exhibit higher glass transition temperature as comparing with that of pure polyimide. The decrease of infrared emissivity of composite films might result from the

absorption of nanostructure pores in S-HMS-EE on energy emitted by the composite films.

The authors would like to express appreciation to Southeast University Science Foundation for the support of this work.

## References

- [1] P. Judeinstein, C. Sanchez, *J. Mater. Chem.* 6 (1996) 511–525.
- [2] K.A. Carrado, *Appl. Clay Sci.* 17 (2000) 1–23.
- [3] Y.F. Lu, Y. Yi, A. Alan, M.C. Lu, J.M. Huang, H.Y. Fan, R. Haddad, G. Lopez, A.R. Burns, D.Y. Sasaki, J. Shelnett, C.J. Brinker, *Nature* 410 (2001) 913–917.
- [4] P.T. Tanev, T.J. Pinnavaia, *Science* 267 (1995) 865–867.
- [5] I.F.J. Vankelecom, S.V.D. Broeck, E. Merckx, H. Geerts, P. Grobet, J.B. Uytterhoeven, *J. Phys. Chem.* 100 (1996) 3753–3758.
- [6] P.T. Tanev, J. Pinnavaia, *Science* 271 (1996) 1267–1320.
- [7] L. Mascia, A. Kioul, *Polymer* 36 (1995) 3649–3659.
- [8] C.J. Cornelius, E. Marand, *Polymer* 43 (2002) 2385–2400.
- [9] G. Leftherioties, P. Yianoulis, *Solar Energy Mater. Solar Cells* 58 (1999) 185–197.
- [10] Q. Xu, W. Chen, R.Z. Yuan, *J. Wuhan University of Technology–Mater. Sci. Ed.* 15 (2000) 15–20.
- [11] P.K. Biswas, A. De, N.C. Pramanik, P.K. Chakraborty, K. Ortner, V. Hock, S. Korder, *Mater. Lett.* 57 (2003) 2326–2332.
- [12] B.P. Lin, H.J. Liu, S.X. Zhang, C.W. Yuan, *J. Solid State Chem.* 177 (2004) 3849–3852.